ZERO-POWER SENSORS WITH NEAR-ZERO-POWER WAKEUP SWITCHES FOR RELIABLE SENSOR PLATFORMS

Visarute Pinrod, Leanna Pancoast, Benyamin Davaji,
Sunwoo Lee, Robin Ying, Alyosha Molnar, and Amit Lal
School of Electrical and Computer Engineering, Cornell University, Ithaca, NY, USA

ABSTRACT

The near zero-power sensor node solution is presented with piezoelectric sensors and DC tunable threshold electrostatic switches. A sensor suite measuring acceleration, rotation, and magnetic field based on PZT lateral bimorphs is used with NEMS switches for the detection of a desired signal pattern and generating a wake up trigger. The sensors are capable of detecting physical signals from 5 Hz to 1.5 kHz, with sourcing load capacitances as high as 200 pF. The sensor sensitivities achieved are: 0.1 V/g for the accelerometer, 31 mV/Gauss for the magnetic field, and 0.31 mV/(◦/s) for rotation. NEMS switches, with threshold voltages in the mV to 15V range, can combine multiple sensor outputs through multi-gate actuation to detect desired event specific features. Using the sensors, we demonstrate the detection of a portable electrical generator in its different operational modes (On/Off state and the Eco mode).

INTRODUCTION

Sensor node reliability is limited by the longevity of the energy sources used to power them [1]. In order to have sensor nodes operational for extended periods of time, power consumption has to be minimized. The power consumed by the sensors of the sensor node is especially critical because the sensors must operate all the time, and generate wakeup trigger for the digital and communication components. MEMS sensors made of piezoelectric materials hold the promise of sensing signals without *any* power consumption, owing to charge being generated as a result of strain in the materials [2]. At the same time, the zero power sensors can trigger near-zero power consuming electrostatic switches that in turn generate a digital trigger as shown in Fig. 1 [3].

Passive filter networks and multi-gate NEMS switches can provide a weighted combination of sensor outputs to allow the tuning of the system for identification of a desired signal pattern. In this work, a combination of the piezoelectric inertial and magnetic sensors with a multi-gate NEMS lateral switch is used to generate a wake-up trigger, thus proving a key component of advanced near-zero power consuming sensor nodes.

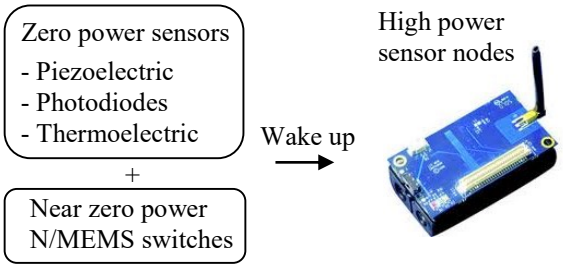

Figure 1: Zero power low-accuracy multi-sensor suite with near zero power N/MEMS switches wake up high power sensor nodes with higher accuracy sensors, communications, and computation, saving battery energy increasing sensor node lifetime.

PZT INPLANE BIMORPH

Fabrication

A 2.54X2.54cmX500 µm APC International bulk PZT plate with silver electrodes on top and bottom is UV laser micromachined (LPKF Protolaser U) to make lateral bimorphs. The bimorphs form as transducers in sensors with lateral features as small as 150 µm [4]. Cutting through PZT substrate defines the beam and the proof mass structures, while removing only the top silver electrode defines the sense electrodes and wire bond pads. A cross section of a PZT bimorph cantilever with thickness t and polarization $\vec{P}$ is shown in Fig. 2a, where two electrodes are defined on the top for sensing while the bottom electrode is grounded. A particular advantage of this technology is the ability to get very low resonance frequencies in tune with the environmental signals, due to the large proof masses. Furthermore, the high electromechanical coupling of PZT ensures energy in signals is transferred to the electrical domain with high efficiency. Lateral motion enables many sensors to be integrated in one PZT plate for high density sensor integration.

Sensing Bimorph

The accelerometer, magnetometer, and rotation sensors in this paper are based off of an in plane bimorph cantilever, which senses in-plane bending. The top view of the cantilever is shown in Fig. 2b. Out-of-plane (z-direction) bending is not sensed because it does not create a net charge on the electrodes. The in-plane longitudinal stress creates common mode charge on +V and -V electrodes, which can be eliminated by differential measurement.

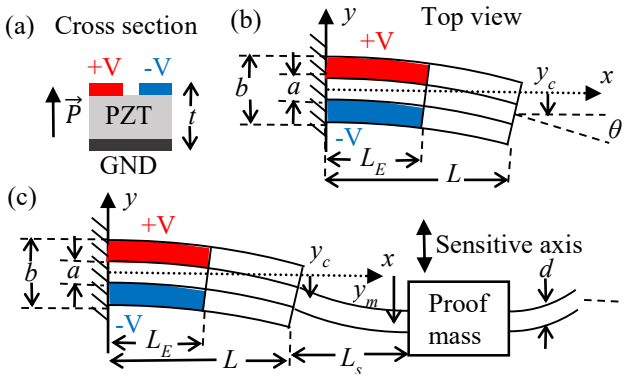

Figure 2: (a) PZT in-plane sensing bimorph cantilever cross section. The bottom electrode is grounded, and top electrodes are outputs. (b) Top view of the sensing cantilever (c) Top view of the sensing cantilever with spring in a clamped-guided configuration.

The output voltage is determined by the charge buildup on the electrodes from the stress on the cantilever. Stress distribution at location (x,y) on the bending cantilever in Fig. 2b when force F is applied on the cantilever tip in $-y$ direction causing y_c tip displacement is

$$T_1(x,y) = \frac{M(x)y}{I} = \frac{F(L-x)y}{I} = \frac{y_c}{k_c}\frac{(L-x)y}{I} \quad (1)$$

where T is the stress, M is the bending moment, $I = \frac{tb^3}{12}$ is the second moment of inertia, t is PZT plate thickness, L is cantilever length, $k_c = \frac{3EI}{L^3}$ is cantilever spring constant, and E is Young modulus [5-6].

The electric displacement D without external electric field is

$$D_z = d_{31}T_1 = d_{31}\frac{y_c(j\omega)}{k_c}\frac{(L-x)y}{I} \quad (2)$$

where d_{31} is a piezoelectric charge constant.

Using Gauss's law, the charge on +V electrode is

$$Q(j\omega) = \int D_z\, dA_z = \frac{y_{c(j\omega)}}{k_c}\frac{d_{31}}{I}\left(LL_E - \frac{L_E^2}{2}\right)\frac{1}{8}(b^2-a^2) \quad (3)$$

where dimension variables are shown in Fig. 2b. The charge on the -V electrode is $-Q(j\omega)$.

The generated charge Q can be measured by a charge integration circuit or a voltage buffer circuit. In this paper, sensors are measured using TL082 JFET differential opamp with input impedance 100 MΩ for sensitivity calibration. Fig. 3a shows circuit model for the +V electrode coupled with an opamp. The output voltage is given by

$$V_{out+}(j\omega) = \frac{Q_+}{C_T}\frac{j\omega R_T C_T}{j\omega R_T C_T + 1} \quad (4)$$

where Q_+ is the charge on +V electrodes, R_T is total resistance, C_T is total capacitance. The output voltage is read out from a differential amplifier $V_{out+} - V_{out-}$. The sensor output passively drives filter network and NEMS switch (Fig. 3b) in the zero power configuration.

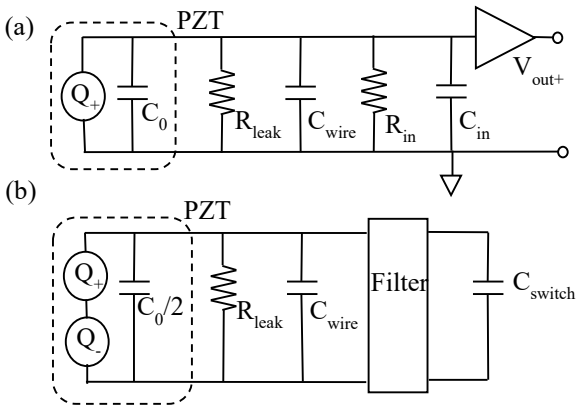

Figure 3: (a) Circuit model for piezoelectric cantilever driving opamp for sensor calibration (b) Circuit model for piezoelectric cantilever drives NEMS switch via filter for zero power application.

Sensing Bimorph with Spring

Constraining a proof mass in a clamped-clamped configuration with many sensing beams reduces cross axis sensitivity. Sensing beams in this configuration are in a clamped-guided beam (Fig. 2c). However, a uniform piezoelectric beam in a clamped-guided beam configuration will produce opposite charge for the halves closest to the anchor and proof mass. Separated electrodes on each half can be used, but extra routing would be needed. Alternatively, smaller spring with height d length L_s can be added between the cantilever tip and proof mass as shown in Fig. 2c. In order to maximize bending moment, the length of the spring is chosen to match the angle at the tip

$$\theta = \frac{F}{EI}\frac{L^2}{2} = \frac{6FL^2}{Etb^3} = \frac{6FL_s^2}{Etd^3} \quad (5)$$

where dimension variables are shown in Fig. 2c. The condition leads to the length of the spring,

$$L_s = L(d/b)^{3/2} \quad (6)$$

The displacement of the sensing cantilever is reduced from the displacement of the proof mass resulting in

$$y_c = \frac{y_m}{1+(d/b)^{3/2}} \quad (7)$$

ACCELEROMETER

The accelerometer design consists of 16 sensing bimorphs. A photograph of a fabricated sensor is shown in Fig. 4a. The sketch for accelerometer electrode combination is shown in Fig. 4b. The equation of motion is given by

$$m\,\ddot{y}_f = m\,\ddot{y}_m + b\dot{y}_m + ky_m \quad (8)$$

where m is the total proof mass, y_m is proof mass displacement in the y (sensitive) direction relative to a frame. $\ddot{y}_f$ is acceleration of the frame, b is damping coefficient, k is total spring constant. Equation 8 can be solved in a frequency domain and get the proof mass displacement

$$y_m = \frac{m}{k}\frac{\omega_0^2}{-\omega^2 + 2j\gamma\omega_0\omega + \omega_0^2}\ddot{y}_f \quad (9)$$

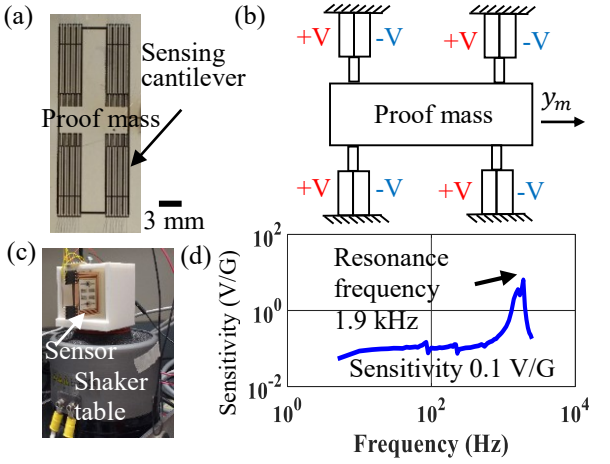

Figure 4: (a) Photograph of PZT accelerometer (b) Sketch of simplified model (c) Photograph of accelerometer calibration on VR shaker table (d) Bode plot sensitivity of accelerometer.

where $\omega_0 = \sqrt{\frac{k}{m}}$ is the resonance frequency of the spring mass system and $\gamma = \frac{B}{2\sqrt{km}}$ is the damping ratio.

By design, spring constant is 28.4 kN/m, proof mass is 290 mg, and resonance frequency is 1.5 kHz. Accelerometer is calibrated by mounting on a Vibration Research (VR) shaker table with 3D-printed holder (Fig. 4c). Measured accelerometer flat band sensitivity is 0.1 V/G with resonance frequency 1.9 kHz (Fig. 4d).

MAGNETOMETER

Magnetometers are made by bonding two permanent magnets, pointing in opposite directions, on two separate clamped-clamped PZT beams (Fig. 5a). The magnetometer schematic is shown in Fig. 5b. Two permanent magnets are attached, on two separate clamped-clamped beams, pointing in opposite directions to cancel out torque caused by rotation.

Force and torque on permanent magnet in an external magnetic field B are

$$\vec{F} = \nabla(\vec{m}_s \cdot \vec{B}) \quad (10)$$

$$\vec{\tau} = \vec{m}_s \times \vec{B} \quad (11)$$

where $\vec{F}$ is the force on sensing magnet, $\vec{m}_s$ is total magnetic dipole moment of a magnet, and $\vec{\tau}$ is the torque applied on the magnet. Since magnetic force (Eq 10) can only measure the gradient of a magnetic field, we take advantage of torque producing a linear response to any magnetic field. The sensitive direction of the assembled magnetometer is perpendicular to the magnet north-south axis. Connecting electrodes as shown in Fig. 5b cancels out

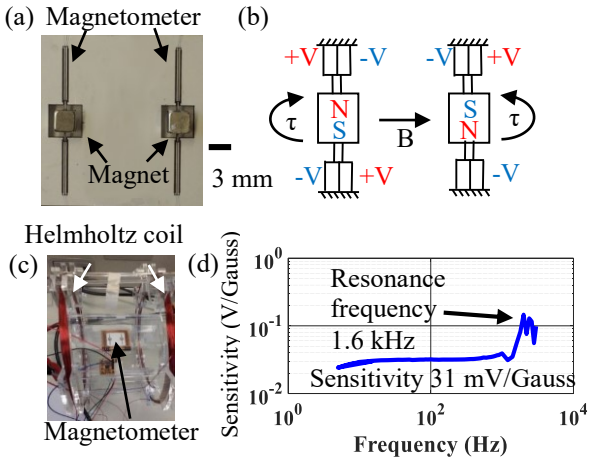

Figure 5: (a) Photograph of PZT magnetometer (b) Sketch of magnetometer (c) Magnetometer calibration setup with Helmholtz coil (d) Bode plot sensitivity of magnetometer.

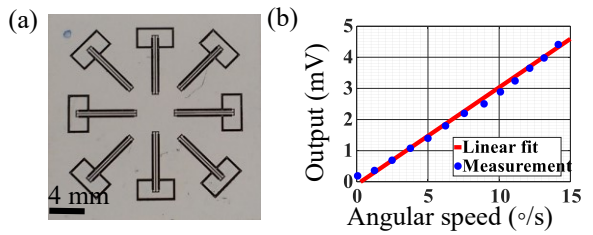

Figure 6: (a) Photograph of PZT rotation sensor (b) Plot of sensitivity calibration on Acutronic BD122 rate table at 30 Hz angular dither.

the linear and angular acceleration, and makes the output proportional to the magnetic field alone.

The photograph of our measurement setup is shown in Fig. 5c. The magnetometer is calibrated by a Helmholtz coil with 100 turns on each coil. The spacing between coils and coil radius is 10 cm. The coil is driven by an Agilent 33500B function generator. The sensitivity measurement is calibrated by a commercial TI DRV425 fluxgate magnetic-field sensor. The calibrated sensitivity is shown in Fig. 5d. The flat band sensitivity is 31 mV/Gauss, the resonance frequency is 1.6 kHz, and the high pass pole is 10 Hz.

ROTATION SENSOR

A set of eight bimorphs and proof masses are connected to obtain a zero power rotation sensor (Fig. 6a) by measuring the angular acceleration during rotation. The geometry and the electrical configurations cancel the cross-axis coupling while maximizing sensitive axis output without active amplifications. Rotation induced acceleration on the proof mass is given by

$$y_m(j\omega) = \frac{m}{k} \frac{\omega_0^2}{-\omega^2 + 2j\gamma\omega_0\omega + \omega_0^2} j\omega\, \Omega R \quad (12)$$

where Ω is the external rotation rate, R is the radius of the sensor proof mass measured from the sensor center. The rotation sensor is calibrated on Acutronic BD122 rate table at 30 Hz. The sensitivity is 0.3 mV/(°/s) (Fig. 6b).

NEAR-ZERO POWER WAKEUP SWITCH

The NEMS switches used to detect the signals are laterally actuated electrostatic switches. A single photomask process (Fig. 7a) is used to fabricate the NEMS switches on SOI substrate, where the patterned structures are etched by reactive ion etching (RIE) and released by vapor HF, followed by a metal deposition for reliable switching.

A completed switch is shown in Fig. 7b. Multiple sized gates are used to actuate the switch to enable a lower turn on voltage and weighing of input signals [3]. Initial testing shows a turn on voltage of 14.36 V and turn off voltage of 14.08 V when actuating with only the largest area gate, shown in Fig. 7c. In the shaker table test, a bias lower than the found turn on voltage is applied to the largest area gate and the sensor is connected to the second largest area gate.

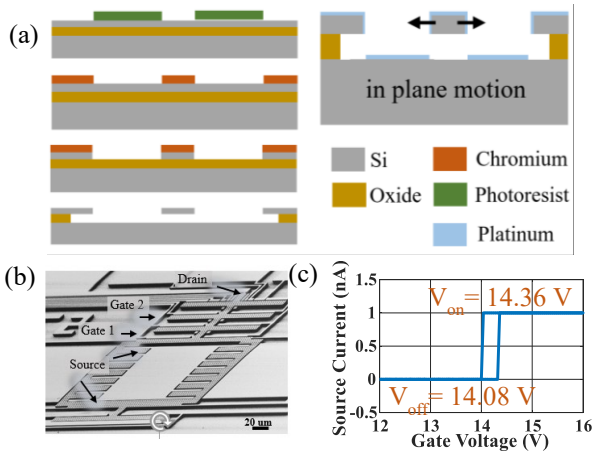

Figure 7: (a) Fabrication process flow (b) SEM image of NEMS switch (c) Switching hysteresis plot.

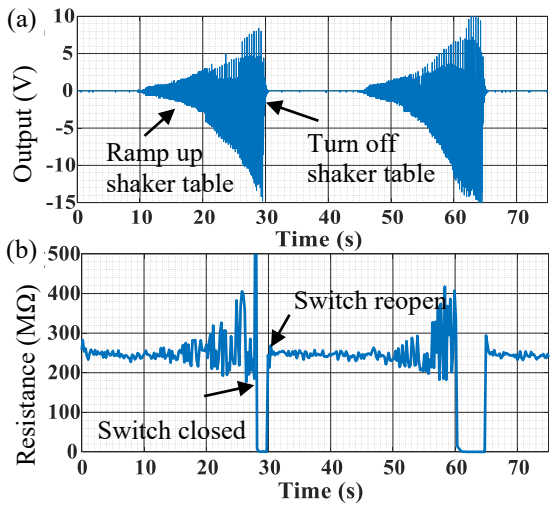

Figure 8: (a) PZT accelerometer output voltage (b) NEMS switch resistance indicating switch close for trigger.

The combined operation of the switch with pre-biased gates generates the digital wake up signal. Fig. 8 shows a z-axis PZT accelerometer with added proof mass, directly coupled to a gate of a pre-biased NEMS switch, closing the switch to generate a wake up signal. The switch was pre-biased at 10V, and the accelerometer was actuated by a shaker table at 280 Hz with an amplitude of 0.12 G. The total power consumption of the wakeup systems is estimated to be <5nW, mainly dominated by the 10V bias power supply leakage current.

FIELD TESTING

In order to measure the efficacy of the zero-power sensor triggered NEMS switches, the fabricated sensors are used to monitor the operation of an internal combustion engine powered portable electrical generator by measuring the physical signals (Fig. 9a). Fig. 9b-c shows the clear frequency signature difference in acquired spectrum signal between different modes.

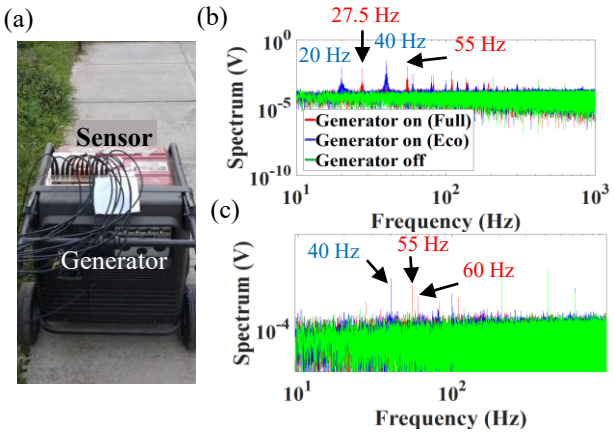

Figure 9: Field test by using zero power sensor for generator detection (a) Photograph of sensors on top of generator (b) Spectrum of PZT accelerometer for generator detection (c) Spectrum of PZT magnetometer for generator detection.

CONCLUSION AND FUTURE WORK

This paper demonstrates piezoelectric zero-power sensors suite fabricated using parallel and series combinations of laser micromachined PZT bimorphs that generate voltages in the millivolt to several volts in the signal range of interest. These voltage levels are sufficient to trigger lateral NEMS switches. This binary trigger based on threshold based activation proves the possibility of a near-zero power wake-up signal for a fully powered sensor suite. The design of acceleration, rotation and magnetic field sensors using the lateral bimorphs are based on a monolithic sensor technology that can be used to make compact sensor systems.

In future, a greater number of sensors will be integrated with multi-gate lateral NEMS switches to detect a pattern of interest. The multi-gate NEMS switch allows different combinations of sensors to best detect desired features. Furthermore, the sensors output can be weighted using a passive filter network to tune the sensitivity of the system. The co-design of sensors and the weights together will extend the range of detection of the sensor node.

ACKNOWLEDGEMENTS

We acknowledge Defense Advanced Research Projects Agency (DARPA), NZERO program, for funding this work. This work was performed in part at the Cornell NanoScale Facility, a member of the National Nanotechnology Coordinated Infrastructure (NNCI), which is supported by the National Science Foundation (Grant ECCS-15420819). This work made use of the Cornell Center for Materials Research Shared Facilities which are supported through the NSF MRSEC program (DMR-1120296). This work made use of the Nanobiotechnology Center shared research facilities at Cornell. We acknowledge Dr. Kwame Amponsah of Xallent LLC for advice about switch fabrication. We acknowledge Jiahao Zhang for monitoring field test.

REFERENCES

[1] J. Yick, B. Mukherjee, and D. Ghosal. "Wireless sensor network survey," *Computer networks* 52, no. 12 (2008): pp 2292-2330.

[2] S. K. Gupta, V. Pinrod, S. Nadig, B. Davaji and A. Lal. "Vibration Powered RF-Transponder for Sensing Low Frequency Motion Events," *PowerMEMS* 2016.

[3] K. Amponsah, N. Yoshimizu, S. Ardanuc, and A. Lal, "Near-kT switching-energy lateral NEMS switch," *IEEE NEMS 2010*, pp. 985-988.

[4] S. Nadig, S. Ardanuç, and A. Lal, "Planar laser-micro machined bulk PZT bimorph For in-plane actuation," *IEEE ISAF/PFM 2013*, pp. 152-155.

[5] V. Kaajakari, *Practical MEMS*, 1st ed. [Las Vegas, Nev.]: Small Gear Pub., 2009.

[6] J. Yu, and C. Lan, "System modeling of micro-accelerometer using piezoelectric thin films", *Sensors and Actuators A: Physical* 88, Issue 2, 15 February 2001, pp. 178-186.

CONTACT

V. Pinrod, vp239@cornell.edu